IMPROVEMENTS TO THE SiO_2 EQUATION OF STATE WITH SHOCK AND POST-SHOCK TEMPERATURES.

Kaitlyn M. Amodeo[1], Erik J. Davies[2], Dylan K. Spaulding[1], Sarah T. Stewart[1], [1]Department of Earth and Planetary Sciences, University of California, Davis, CA 95616 (kamodeo@ucdavis.edu), [2]Lawrence Livermore National Laboratory, Livermore, CA 94550

Introduction: Planet formation and evolution involves high energy impacts capable of melting and vaporizing silicate mantles [1, 2]. Wide-ranging equations of state (EOS) that accurately capture the temperatures along the shock Hugoniot and in the post-shock state are necessary to understand the material behavior occurring in natural phenomena. SiO_2 is an important end-member phase and frequently used as an *in situ* reference material for experiments, but researchers lack accurate wide-ranging EOS models for quartz and fused silica (amorphous SiO_2), particularly where these materials undergo shock melting.

Along with their utility as compositional end-member minerals, quartz and fused silica are often used in a variety of shock experiments as windows and standards for thermal emission and impedance matching [3, 4]. Thus, improving the laboratory measurements and modeled data for these materials provides better standard references. Previous studies using gas guns [5, 6] and laser-driven shocks [3] sampled this region, but little data is available in the superheating region of the Hugoniot and liquid region along the vapor curve. Additional data in this region provides insight to both the transition of SiO_2 into the liquid phase in a shocked state as well as the onset of melting and vaporization upon release.

The analytic equations of state code package (ANEOS) is frequently used by the planetary science community as it is capable of spanning the substantial temperature and pressure range achieved in natural impact phenomenon [7]. The code package has multiple features that enable modeling of solids, liquids, gases, and plasmas. For most natural materials, the code package cannot accurately model the entire pressure-temperature range needed. As a result, each developer must make decisions about which features to use in the code package and which regions to fit more accurately.

Melosh [7] made updates to ANEOS using SiO_2 where a Mie-type potential is used for the solid phase and molecular clusters are used for the vapor phase (M-ANEOS). At present, the available ANEOS models for silica have significant discrepancies in the melt region and liquid-vapor phase boundary compared to laboratory observations. Figure 1 shows currently available ANEOS model Hugoniot and vapor domes for SiO_2 alongside lab data [6, 8, 9].

This study focuses on measuring shock and post-shock temperatures of quartz and fused silica in the pressure range where these materials undergo superheating and melting, approximately 55-130 GPa using multiple pyrometry systems. Here, we describe our shock pyrometry experiments on fused silica as well as plans for improving the model equation of state.

Methods: Shock data were collected at the UC Davis Shock Compression Laboratory using the 80/25 mm two-stage light gas gun. This facility is capable of producing high-precision planar shock waves though geologic materials at impact velocities up to $\sim$ 7 km s^{-1} or $\sim$ 130 GPa in silica.

Specialized optical pyrometry and velocimetry diagnostics allows us to measure impact velocity, shock ve-

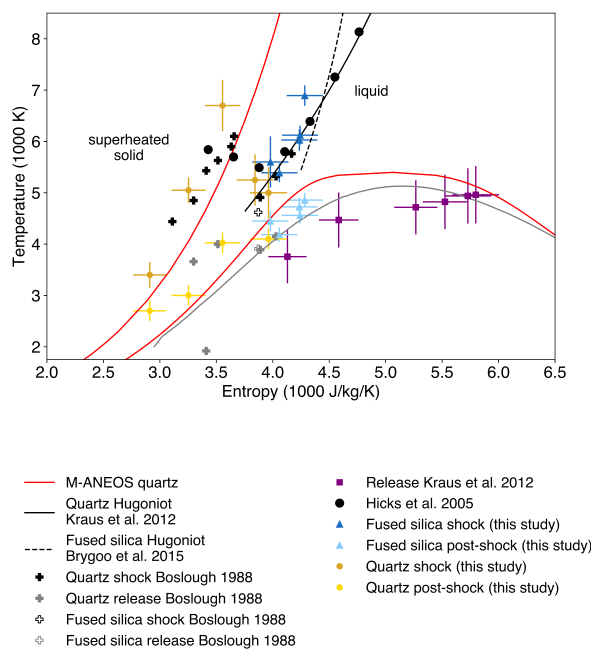

Figure 1: Plot of shock Hugoniots and the vapor dome for silica: M-ANEOS Hugoniot from Melosh [7] (red solid lines), quartz Hugoniot and vapor dome from Kraus et al. [9] (solid black and gray lines, purple squares), and fused silica Hugoniot using entropy from Kraus et al. [9] and temperatures from Brygoo et al. [10] (dashed black line). Notably, the model Hugoniots do not include the melt curve or the superheating phenomenon. Decaying shock data from Hicks et al. [3] follow the liquid Hugoniot and potentially follows the same superheating pattern, but this transition is not well resolved in decaying shock experiments.

locity, and shock/post-shock temperatures [11]. A typical sample is a 25 mm diameter disk with a thickness of 3 mm and an average density of 2.181 ± 0.002 g/cc for fused silica and 2.651 ± 0.002 g/cc for quartz. The samples are mounted in a secondary vacuum chamber to avoid contamination of spectral radiance data from residual shocked gas in the gun's target tank.

Temperature was measured using three distinct fiber-coupled pyrometry systems. The first system consists of four near-infrared (NIR) InSb detectors centered at 1.8, 2.3, 3.5, and 4.8 μm. Next, are two visible light detectors (Si photodiodes), with a 600 nm long pass filter and a 700 nm short pass filter. The third is a Streaked Visible Spectroscopy (SVS) system covering a broad, continuous spectrum of visible wavelengths from 350 to 850 nm [12]. The time-dependent thermal emission data are analyzed as described in Luo et al. [8] which corrects the spectral radiance for wavelength-dependent absorption. The combination of these systems allows us to determine calibrated shock and post-shock radiance over a broad wavelength range that are converted to temperature with the Planck function.

ANEOS improvements: The improvements to ANEOS follow those described in [13] in which the forsterite EOS was improved using additional lab data. These improvements include the addition of a user adjustable heat capacity; the original heat capacity in ANEOS asymptotes to $3N_0kT$, or the classical Dulong-Petit limit. This limit is appropriate for the solid phase, but is not appropriate for the melt or supercritical fluid. As shown in Fig. 1, the M-ANEOS Hugoniot from [7] is in fairly good agreement with quartz shock temperature measurements [6] in the superheated regime. However, there is strong disagreement with this Hugoniot and the shock temperature data inferred to be in the liquid field (those points at higher specific entropies).

With the updated ANEOS code package, the heat capacity can now be adjusted with an empirical term f_{cv} such that the limiting heat capacity is $3f_{cv}N_0kT$. Currently, changing this term leads to a poorer quality fit in the solid region. Future work will use the ANEOS package to make multi-phase EOS tables that use the appropriate thermal models for the solid and fluid phases.

Preliminary results: A preliminary data set is shown in Fig. 1. Our data clearly display the superheating sawtooth pattern of a metastable stishovite phase (up to ∼ 3.6 kJ/kg/K), best correlating with the M-ANEOS curve, followed by a drop in temperature as these materials undergo shock melting. Our shock temperature data are slightly offset from the Hugoniot and vapor dome predicted by [9] but have a better fit to the Hugoniots for shock melted silica past 3.6 kJ/kg/K. Including the new post-shock temperature data, we will be able to further improve the liquid-vapor boundary model. The combination of shock temperatures with static thermodynamic data will be used to improve the calculation of entropy on the Hugoniot.

In the data shown in Fig. 1, the post-shock temperatures assume an emissivity of 1; however we infer wavelength dependence on this parameter. We note that in previous work, the inferred shock front emissivity varied noticeably between experiments [5]. Inclusion of infrared wavelengths in thermal radiance measurements indicates that the uncertainties in the inferred temperature are larger than typically reported for shock temperature measurements using visible data alone. Our measured radiance in silica over the entire visible to near-infrared range cannot be fit by an ideal greybody. We infer the presence of wavelength-dependent material properties that introduce additional uncertainties into the inference of the sample temperature. These uncertainties are reflected in our error bars.

Conclusion: Shock and post-shock temperature data for quartz and fused silica can provide extremely useful thermodynamic data that are needed to improve equation of state models over the wide range of pressures and temperatures attained in planetary impacts. Adjustments to the user defined heat capacity along with updated temperature measurements around the solid-liquid phase boundary in ANEOS will create a better EOS model for silica melt.

Acknowledgements: Portions of this work were supported by NASA grant NNX15AH54G, Simons Foundation grant 55420, DOE-NNSA grant DE-NA0003842, NASA grant NNX16AP35H (EJD), and LLNL under Contract DE-AC52-07NA27344 (EJD).

References: [1] Chambers J. (2010) *Exoplanets*, 23. [2] Canup R. M. (2008) *PTRS*, *366*, 4061. [3] Hicks D. G. et al. (2005) *Physics of Plasmas*, *12*, 082702. [4] Knudson M. D. and Desjarlais M. P. (2009) *PRL*, *103*, 225501. [5] Lyzenga G. A. and Ahrens T. J. (1980) *GRL*, *7*, 141. [6] Boslough M. B. (1988) *JGR*, *93*, 6477. [7] Melosh H. J. (2007) *MAPS*, *42*, 2079. [8] Luo S. N. et al. (2004) *JGR: Solid Earth*, *109*. [9] Kraus R. G. et al. (2012) *JGR: Planets*, *117*, 22. [10] Brygoo S. et al. (2007) *Nature Materials*, *6*, 274. [11] Stewart S. T. and Spaulding D. K. (2017) *LPSC XLVIII* 2154. [12] Davies E. J. et al. (2020) *AIP Conf. Proc. SCCM19*, 060008. [13] Stewart S. et al. (2020) *AIP Conf. Proc. SCCM19*, 080003.